August 1972 Solar-Terrestrial Events: Observations of Interplanetary Shocks at 2.2 AU

EDWARD J. SMITH,[1] LEVERETT DAVIS, JR.,[2] PAUL J. COLEMAN, JR.,[3] DAVID S. COLBURN,[4] PALMER DYAL,[4] AND DOUGLAS E. JONES[5]

Pioneer 10 magnetic field measurements, supplemented by previously published plasma data, have been used to identify shocks at 2.2 AU associated with the large solar flares of early August 1972. The first three flares, which gave rise to three forward shocks at Pioneer 9 and at earth, led to only a single forward shock at Pioneer 10. The plasma driver accompanying the shock has been tentatively identified. A local shock velocity at Pioneer 10 of 717 km/s has been estimated by assuming that the shock was propagating radially across the interplanetary magnetic field. This velocity and the rise time of $\simeq 2$ s imply a shock thickness of ~ 1400 km, which appears to be large in comparison with the characteristic plasma lengths customarily used to account for the thickness of the earth's bow shock. This Pioneer 10 shock is identified with the second forward shock observed at Pioneer 9, which was then at 0.8 AU and radially aligned with Pioneer 10, since it was apparently the only Pioneer 9 shock that was also driven. The local velocity of the Pioneer 9 shock of 670 km/s, previously inferred by other authors, compares reasonably well with the local velocity at Pioneer 10, but both values are significantly smaller than the average value computed from the time interval required for the shock to propagate from the sun to Pioneer 9 (2220 km/s). The velocity implied by the time required to propagate from Pioneer 9 to Pioneer 10 (770 km/s) is in reasonable agreement with the local velocities. The fourth solar flare also gave rise to a forward shock at Pioneer 10 as well as at Pioneer 9. The local velocity at Pioneer 10, estimated on the basis of quasi-perpendicularity, is 660 km/s, a value which again agrees well with previously derived velocities for the Pioneer 9 shock of 670 km/s. The local velocities for this shock and the velocity between Pioneer 9 and Pioneer 10 (635 km/s) are also significantly less than the average velocity of propagation from the sun to Pioneer 9 (830 km/s). The general finding that the local velocities of both shocks are approximately equal at 0.8 and 2.2 AU but significantly slower than the average speeds nearer the sun is interpreted as evidence of a major deceleration of the shocks as they propagate outward from the sun that is essentially completed when the shocks reach 0.8 AU, there being little, if any, subsequent deceleration. This conclusion is qualitatively inconsistent with previous inferences of a deceleration of the shocks as they propagate from 0.8 to 2.2 AU. A third, reverse shock is also identified in the Pioneer 10 data which was not seen either at Pioneer 9 or at earth. The estimated speed of this shock is 530 km/s, and its estimated thickness is $\lesssim 500$ km, which compares well with an anticipated proton inertial length of 500 km.

INTRODUCTION

The solar-terrestrial events of early August 1972 provide a unique opportunity to investigate the response of the interplanetary medium to large solar flares. Within a few days, several large flares occurred in McMath plage region 11976. One of these flares produced the largest solar proton event ever observed at earth, and four produced interplanetary shocks and gave rise to widespread interplanetary and terrestrial disturbances, including geomagnetic storms, aurorae, and cosmic ray decreases [*World Data Center A for Solar-Terrestrial Physics*, 1973].

This remarkable episode of solar activity was observed by space experiments under particularly favorable circumstances. Measurements of magnetic fields, plasma, and energetic particles were made not only near earth but also at two Pioneer spacecraft (9 and 10) that were nearly radially aligned at 0.8 and 2.2 AU (Table 1). The properties of the interplanetary medium during this interval are intimately related to various energetic particle effects, such as the propagation of particles from the sun throughout the solar system, the local acceleration of particles by interplanetary shocks, and Forbush decreases in the cosmic ray flux. The availability of simultaneous data at widely separated points also makes it possible to study the propagation of interplanetary shocks over large heliocentric distances.

Since it first became possible to detect shocks in interplanetary space with satellites and space probes [*Sonett et al.*, 1964], it has become evident that deceleration is a common feature of the propagation of shocks from the sun to $\simeq 1$ AU [*Gosling et al.*, 1968; *Hundhausen*, 1970]. *Hundhausen* [1972, pp. 171–177] gives a table of velocities for interplanetary shocks observed between 1962 and 1969. The local velocities derived from plasma and magnetic field measurements are typically smaller than the velocities implied by the transit times from the sun to the spacecraft. *Hundhausen* [1972] summarizes the situation by pointing out that the mean shock speed derived from satellite measurements is $\simeq 500$ km/s, while the average transit velocity implied by flare-shock associations is $\simeq 730$ km/s. In addition, *Chao and Lepping* [1974] have shown that the most probable transit speed is $\simeq 650$ km/s, a value also significantly greater than the mean or most probable local speed.

The propagation of flare-associated shocks has been studied theoretically beginning with *Parker* [1961] and more recently by using numerical simulation (see the reviews by *Hundhausen* [1972] and Dryer [1975]). *Hundhausen and Gentry* [1969] simulated the propagation of shocks from the sun to 1 AU through the ambient solar wind and found a progressive deceleration with increasing radial distance. *Hundhausen* [1973] also specifically investigated the evolution of shocks beyond 1 AU and again found a gradual deceleration. The simulation showed that shocks associated with small mass or momentum input into the solar wind by the flare were decelerated most strongly.

Prior to the launch of Pioneer 10, in situ observations of

[1] Jet Propulsion Laboratory, Pasadena, California 91103.
[2] California Institute of Technology, Pasadena, California 91125.
[3] University of California, Los Angeles, California 90024.
[4] NASA Ames Research Center, Moffett Field, California 94035.
[5] Brigham Young University, Provo, Utah 84602.

Paper number 6A0780.

TABLE 1. Identification Times of August 1972 Events

	Event 1		Event 2		Event 3		Event 4	
	Time, UT	Date	Time, UT	Date	Time, UT	Date	Time, UT	Date
Flares	0316	Aug. 2	1959	Aug. 2	0621	Aug. 4	1505	Aug. 7
Pioneer 9 shocks	0420	Aug. 3	1117	Aug. 3	2323	Aug. 4	0707	Aug. 9
Shocks at earth	0120	Aug. 4	0221	Aug. 4	2054	Aug. 4	2354	Aug. 8
Pioneer 10 shocks	1520	Aug. 6	1540	Aug. 9	0300	Aug. 13		

interplanetary shocks were restricted to the vicinity of 1 AU. Thus the Pioneer 10 observations provide the first opportunity to observe flare-produced shocks at a heliocentric distance significantly greater than 1 AU and to study their propagation with increasing distance. The intensity of the August flares and their production of striking solar-terrestrial effects were fortunate, because uncertainties in the identification of corresponding flares and shocks were minimal. Such uncertainties have often plagued previous shock studies.

There have been several previous attempts to determine the velocities of the August shocks and to investigate their possible acceleration or deceleration as they propagate outward from the sun. *Mihalov et al.* [1974] published the Pioneer 9 plasma and magnetic field parameters during the August events as well as the plasma measurements obtained with Pioneer 10. They identified four shocks in the Pioneer 9 data and obtained a local velocity for the largest shock. *Dryer et al.* [1975] used average velocities of propagation from the sun to Pioneer 9, to earth, and to Pioneer 10 to obtain a preliminary identification of corresponding shocks at the different locations. The behavior of the average velocities as a function of heliocentric distance implied a relatively large and continuous deceleration of the shocks as they propagated outward from the sun. The apparent deceleration beyond 1 AU was so pronounced that *Dryer et al.* [1975] suggested a possible transformation of the shocks in the outer solar system back into large-amplitude hydromagnetic waves. *Zastenker et al.* [1975], using Prognoz 1 and 2 plasma measurements near earth, also attempted to identify corresponding shocks and were similarly led to conclude that the shocks continually decelerated as they propagated outward. Recently, *Dryer et al.* [1976] computed the local velocities of the four Pioneer 9 shocks by carrying out a Rankine-Hugoniot analysis of the simultaneous plasma and field data.

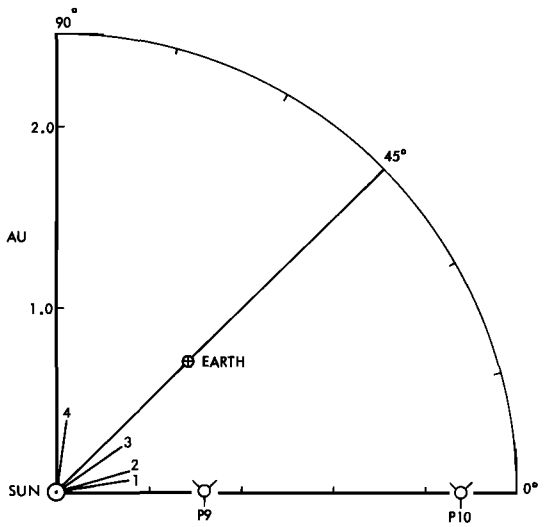

Fig. 1. Relative positions of the earth, Pioneer 9, Pioneer 10, and the solar flares. During early August 1972 the two Pioneer spacecraft were nearly radially aligned, and the direction from the sun to the two spacecraft has been used to define the x axis (or 0° longitude) in this figure. Pioneer 9 was located at 0.78 AU from the sun, and Pioneer 10 was located at 2.2 AU. The Pioneer-sun-earth angle was 45°, as is shown. The radial lines issuing from the sun show the relative longitudes of the four large flares referred to the sun-Pioneer line. The first flare was near central meridian passage as seen by the two spacecraft, while the fourth flare was essentially a west limb flare.

This report presents the magnetic field observations at Pioneer 10, which was then 2.2 AU from the sun in transit to Jupiter. The data are compared with the simultaneous plasma measurements to identify the major flare-induced plasma effects at 2.2 AU, such as shocks, flare ejecta, and high-velocity streams. Estimates of the local speeds of the Pioneer 10 shocks in the solar system inertial frame are derived from the Pioneer 10 magnetic field and plasma velocity measurements and the assumption that the shocks are quasi-perpendicular.

The local shock velocities are compared with average velocities of propagation between the sun and Pioneer 9, between the sun and Pioneer 10, and between the two Pioneer spacecraft as well as with the local velocities at Pioneer 9. Such a comparison cannot be carried out successfully without a proper identification of corresponding shocks at Pioneer 9 and 10. The identification is not a simple matter because more shocks are observed at Pioneer 9 than at Pioneer 10. Our identification is based to a large extent on the observation that the first shock observed at Pioneer 10 is a driven shock rather than a blast wave and that the second shock at Pioneer 9 also appears to be driven. The radial alignment of the two Pioneer spacecraft reduces the likelihood of significant velocity differences arising from nonspherically symmetric shock fronts, i.e., a dependence of velocity on heliographic longitude rather than on radial distance.

OBSERVATIONS

The Pioneer 10 magnetometer and plasma analyzer are improved versions of the Mariner 4 and 5 vector helium magnetometers and the quadraspheric analyzers previously flown on Pioneer 6–9. The Pioneer 10 investigations are described by *Smith et al.* [1975] and *Wolfe et al.* [1974]. During the interval in which the flare effects were observed, both instruments were typically being sampled very rapidly; for example, the magnetic field vector was measured either 16 or 8 times every 3 s. However, some of the analysis reported here is based on averages over ½- or 1-hour intervals. This low time resolution is usually suitable for showing the major large-scale features, such as shocks, associated with the flares.

When the flares occurred, Pioneer 10 was approximately 45° east of the earth-sun line at a heliocentric distance of 2.2 AU (Figure 1). The first two flares, at 0316 UT (1B, E35) and 1958 UT (2B, E28) on August 2, occurred 10° and 17° west of central meridian passage as viewed from Pioneer 10. The third

and fourth flares, at 0617 (3B, E09) on August 4 and at 1449 (3B, W38) on August 7, took place at 35° and 80° west meridian as seen from Pioneer. Thus the flare sequence produced a wide range of different geometries between the flare site and the point of observation.

The magnetic field magnitude and plasma velocity over successive 6-day intervals during August 5–10 (days 218–223) and August 11–16 (days 224–229) are shown in Figures 2 and 3. The hourly values of the solar wind velocity used in these figures were kindly provided by John Wolfe.

Prior to the arrival of the shock on August 6 the average strength of the interplanetary field was only 2.5 γ, a typical value for a heliocentric distance of 2.2 AU. The plasma velocity of 350–400 km/s was also typical of quiet conditions. However, both the magnetometer data of Figure 2 and the plasma data of *Mihalov et al.* [1974] show considerable nonuniformity in this preshock plasma.

At the shock front (event A in Figure 2) the field magnitude jumped abruptly to nearly 10 γ, an increase by a factor of 3, and the velocity rose to a value in excess of 625 km/s. Figure 4 shows the field magnitude in the vicinity of the shock at moderate time resolution (1-min averages). The shock is shown at the highest possible time resolution in Figure 8. The shock arrived at 1520 UT (earth receipt time) and was followed by large, irregular field variations. (The times associated with the Pioneer measurements are the times of receipt of the telemetered data at earth, uncorrected for the one-way light time of 13–15 min.)

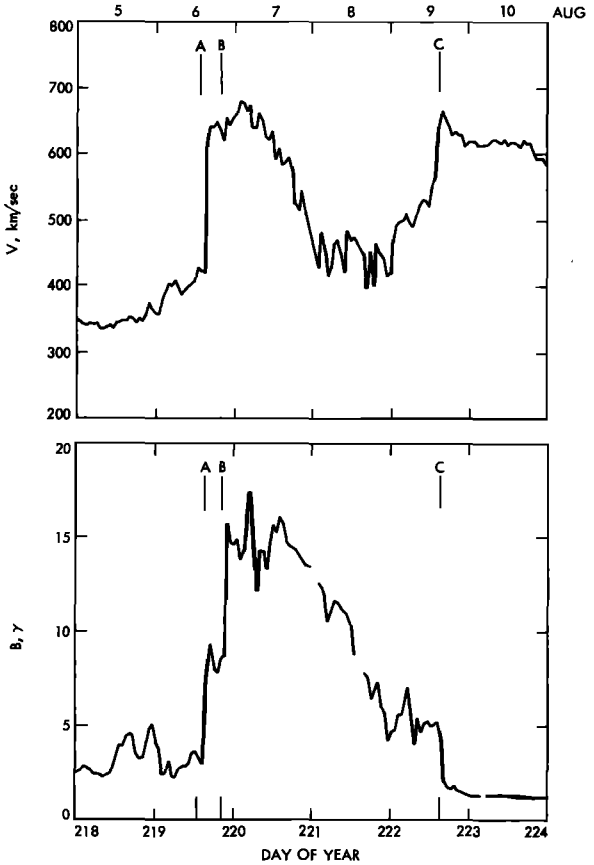

Fig. 2. Pioneer 10 magnetic field and solar wind velocity. (Top) Plot of hourly values of the solar wind speed during August 5–10. (Bottom) Plot of hourly averages of the field magnitude. Event A is a forward shock, event B has been tentatively identified as the plasma driver, and event C is a reverse shock.

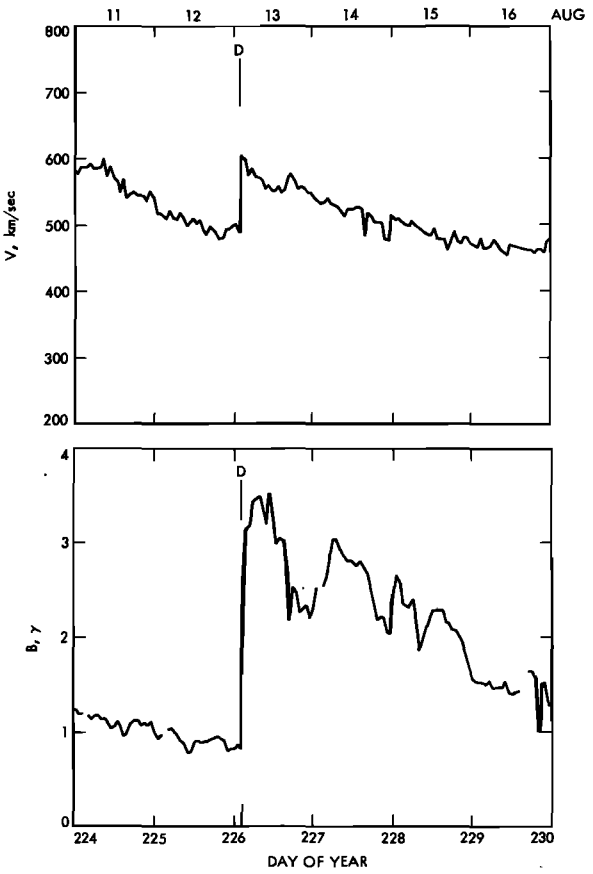

Fig. 3. Pioneer 10 magnetic field and solar wind velocity. The format is the same as that of Figure 2. The data cover the interval August 11–16. Event D is a forward shock.

The gas arriving immediately after the shock was originally preshock solar wind that had been piled up and compressed behind the shock front. For several hours the field magnitude fluctuated irregularly between 5 and 15 γ, presumably partly as a consequence of the compression of the previously existing irregularities by the passage of the shock through this gas. The plasma velocity remained fairly constant at $\simeq$625 km/s during this interval.

At ~2200 UT on August 6 a second abrupt jump in the field (event B in Figure 2, shown at moderate time resolution in Figure 5) occurred, after which the magnitude remained nearly constant for almost a day at a very high level of approximately 16 γ. The plasma velocity remained essentially constant during the large change in field. At the same time the average plasma density was approximately constant, but the temperature dropped abruptly [*Mihalov et al.*, 1974]. High-resolution magnetometer data show that this jump actually occurred at 2205 and was much more gradual than that in typical shocks. This was probably neither a shock (no jump in velocity was observed) nor a rotational discontinuity (the field magnitude underwent a large change). It was more likely a complicated tangential discontinuity, although this surmise has not been verified by analysis.

It is tempting to identify this feature as the arrival at Pioneer 10 of the flare ejecta or plasma driver that was pushing its way through the quiet solar wind preceded by the shocked gas and the interplanetary shock; however, other interpretations are possible, as is discussed below. An alternative identification of the arrival time of the flare ejecta is 0900 hours on August 7

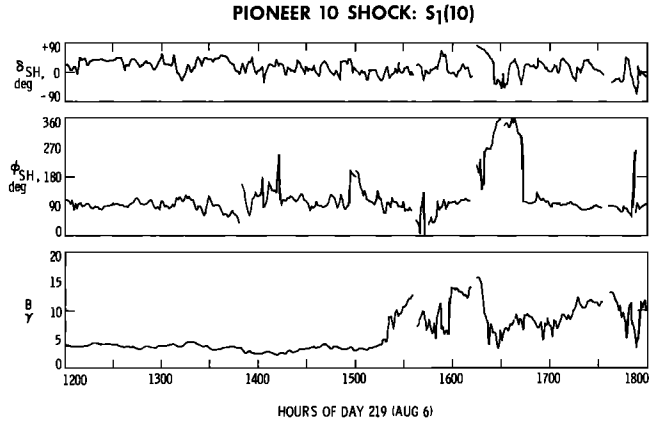

Fig. 4. Pioneer 10 magnetic fields in the vicinity of the first forward shock. One-minute averages of the field magnitude and latitude and longitude, in solar polar coordinates, are shown over a 6-hour interval on August 6 containing the first shock. In solar polar (SH) coordinates the x (or R) axis (corresponding to 0° longitude) is outward from the sun, the y (or T) axis (corresponding to +90° longitude) is parallel to the solar equator and points in the direction of motion of the planets, and the orthogonal z (or N) axis (corresponding to +90° latitude) points northward.

(Figure 6), after which the field changed direction and started a steady decrease in magnitude. Further analysis, including numerical simulations [e.g., *Dryer et al.*, 1976], may reveal which interpretation is correct. In addition, one of these features may prove to be associated with the arrival of solar wind whose helium content is enhanced, a condition which has been suggested as being representative of flare ejecta [*Hirshberg et al.*, 1970].

The wind velocity dropped steadily from a peak value of 680 km/s early on August 7 to a relative minimum of approximately 450 km/s near 1200 on August 8. The field strength dropped steadily from 16 γ at 1500 on August 7 to 11 γ at 1200 on August 8 and continued to drop rapidly to about 5 γ by the end of the day. During the first 15 hours of August 9 the magnetic field strength fluctuated near 5 γ. During this period the plasma data show a gradually rising velocity and a falling temperature [*Mihalov et al.*, 1974]. At 1540, just before the

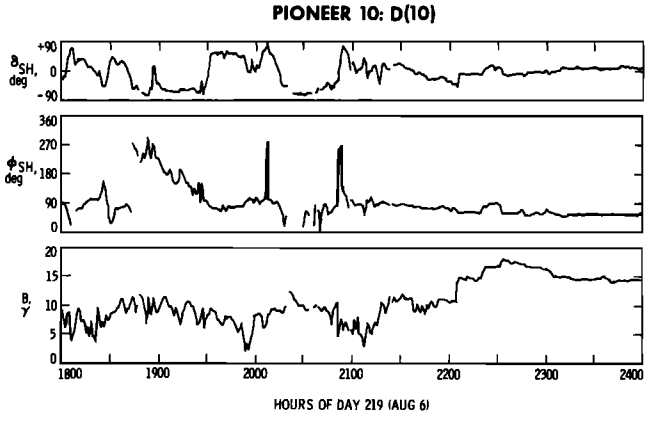

Fig. 5. Pioneer 10 magnetic fields in the vicinity of the discontinuity (D) tentatively identified as the plasma driver. The format is the same as that of Figure 4, and the data cover the succeeding 6 hours. Note the change in the character of the field at 2205, when a discontinuity, tentatively identified as the plasma driver, reached Pioneer 10. The fields preceding the discontinuity are very irregular, as is anticipated for postshock solar wind, but the field following the discontinuity is larger and less irregular in both magnitude and direction.

velocity reached its peak value at Pioneer 10, B decreased abruptly to an average value of 2 γ (event C in Figure 2). This downward jump has the appearance of a reverse shock [*Sonett and Colburn*, 1965; *Burlaga*, 1970].

The magnetic data adjacent to event C are shown at moderate resolution in Figure 7 and at high time resolution in Figure 9. The abrupt transition requires less than 1 s (there are only two magnetic measurements within the transition), and it is thus very thin. The field strength drops to three fifths of its original value without a significant change in the direction of the field. Wavelike quasi-periodic variations in both the field direction and the magnitude are evident. The fluctuation amplitude is enhanced significantly behind the discontinuity.

If this is a reverse shock, the velocity should increase, and the density and temperature decrease. The velocity does rise, and the density and temperature are low (D. Intriligator, private communication, 1976). After the discontinuity the magnetic field has the strength and character of undisturbed solar wind. The presence of waves both upstream and downstream also suggests that this is a shock, such waves having been commonly observed in association with interplanetary as well as planetary shocks [*Fairfield*, 1974]. On the basis of the available data we consider it most likely that this event is a reverse shock that forms at the interface where the low-density plasma in the trailing high-velocity stream is first slowed as it encounters the outer, compressed parts of the preceding stream. Such a reverse shock is moving sunward with respect to the plasma but is convected outward because of the higher velocity of the solar wind.

During the succeeding 6-day interval (August 11–16, shown in Figure 3) the plasma velocity declined steadily for the first 2 days, and the magnetic field was typical of undisturbed conditions. However, before the velocity reached its quiescent value, another possible shock (event D in Figure 3) arrived at Pioneer 10 at approximately 0302 ± 22 min on August 13. Because of an unfortunate data gap from 0241 to 0324, neither the exact time of the event nor positive evidence that it was a shock is available. Nevertheless, its identification as a shock seems quite secure, since all the field and plasma changes are consistent with a fast forward shock. In contrast to event A this shock was followed by a slow monotonic decrease in both B and V following the initial increase. Although interplanetary conditions were disturbed for approximately the same interval of 3 days, this event is much smaller and much simpler than, and lacks most of the features associated with, the earlier forward shock.

Discussion

Shock propagation velocity. Much can be learned by tracing the evolution of a shock from its origin in a particular flare to its passages by Pioneer 9 and 10. However, the association between the various events is often ambiguous and leads to more than one interpretation of the data. Accordingly, we first estimate the local shock velocity at each spacecraft of each shock observed and use this, as well as other features of the shocks, to follow their outward motion through the solar system. Among other things, we consider the possible deceleration of the shocks.

The method used to obtain estimates of the shock velocity with respect to both the solar wind and the solar system inertial frame is based on the conservation of magnetic flux and assumes that the shock is propagated radially and is primarily a perpendicular shock, i.e., that the shock normal is perpendicular to the magnetic field. If subscripts 1 and 2

refer to initial and final conditions, respectively, the shock speed in the inertial frame is given by

$$V_{\text{in}} = (B_2V_2 - B_1V_1)/(B_2 - B_1) \quad (1)$$

The shock velocity in the frame of the preshocked solar wind is then $V_{sw} = V_{\text{in}} - V_1$ for a forward shock and $V_{sw} = V_{\text{in}} - V_2$ for a reverse shock. More accurate values of the shock speed can ultimately be obtained by making a careful analysis based on the Rankine-Hugoniot relations and using both magnetic field and more complete plasma data.

The choice of B and V values to be used in the above equation was carefully coordinated with D. Intriligator, who had high time resolution plasma data available from both Pioneer 9 and Pioneer 10 [*Intriligator*, 1976]. An attempt was made to obtain values adjacent to the shock on both the upstream and the downstream side. Typically, plasma spectra were available every few minutes. The individual velocities adjacent to each shock were inspected to establish that they did not straddle the shock front and that they were representative values.

For most shocks the velocities were sufficiently constant that the values immediately adjacent to the shock were used. In that case the field magnitude was averaged over the corresponding interval of several minutes during which the plasma data were obtained. If the field magnitude was changing over this interval or if much higher time resolution magnetic data were available (as was the case at Pioneer 10), the field magnitude was averaged over intervals of several seconds immediately adjacent to the shock.

For a few shocks the plasma velocity was varying either before or after the shock. In these cases the maximum and minimum values for four successive samples were averaged and used in the calculations in the expectation that this procedure would tend to minimize the deviations between the value used and the unknown correct value.

Shocks are such variable structures that some judgment based on the individual shock is necessary and desirable in order to decide what values of B and V are likely to be representative. After a choice was made, the shock velocity was then recomputed for other possible choices of both B and V in order to establish that no large differences in V_{in} ($\gtrsim$10%) were implied.

Table 2 shows the inertial velocities of the four Pioneer 9 shocks as computed from the above equation and as derived by *Dryer et al.* [1976] from a Rankine-Hugoniot analysis. The observed values of field magnitude and velocity are based on high-resolution field and plasma data (one sample every 18.7 s and 7.5 min, respectively). The two columns of Table 2 displaying the magnetic field magnitudes adjacent to the shocks show the relatively large jumps in field strength that imply quasi-perpendicularity. The table also provides a direct comparison of the two approaches and shows that equation (1), based on quasi-perpendicularity, leads to velocities that are approximately the same as those derived from the Rankine-Hugoniot analysis.

The relative differences between our velocities and the *Dryer et al.* [1976] velocities vary between 0 and 10% for the component of the velocity along the shock normal (V_n) and between 6 and 13% for the radial component of the shock velocity (V_R). Apparently, there is a tendency for the quasi-perpendicularity analyses to underestimate the radial velocity by 10–15%. As will be seen below, uncertainties of this order are only a small fraction of the differences between local and average velocities and hence are not expected to influence our conclusions. For these four cases the Rankine-Hugoniot analyses indicate that the angle between the shock normal and the magnetic field direction varied between 79° and 37°, while the angle between the normal and the radial direction varied between 14° and 31°. According to *Greenstadt* [1974] the earth's bow shock may be classified as being quasi-perpendicular for field-normal angles as small as 50° ± 10°.

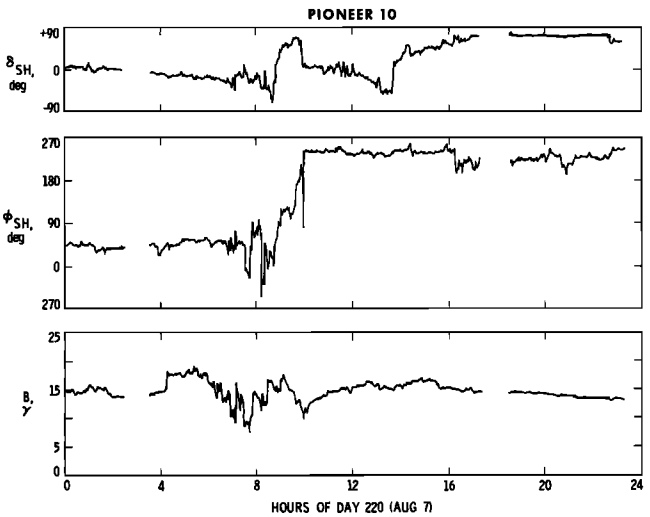

Fig. 6. Pioneer 10 magnetic fields observed on August 7. One-minute averages of the field latitude (δ_{SH}), longitude (ϕ_{SH}), and magnitude (B) are shown for all 24 hours of day 220. The dominant feature is a sector boundary observed at ≃0900. Other features that might be identified with a plasma driver are the increase in B near 0400 and perhaps the abrupt change in δ_{SH} near 1400.

Table 3 shows the corresponding velocities for the three Pioneer 10 shocks. Again, the values of field strength and velocity are based on high-resolution Pioneer 10 data.

The changes in field direction across the first and second (reverse) shocks (Figures 8 and 9) are very small, the included angles between the upstream and downstream fields being only 6° and 2°, respectively. Thus both are nearly perpendicular shocks, as is assumed in (1). The included angles are too small to compute with any degree of certainty the direction of the shock normal by using the coplanarity theorem [*Colburn and*

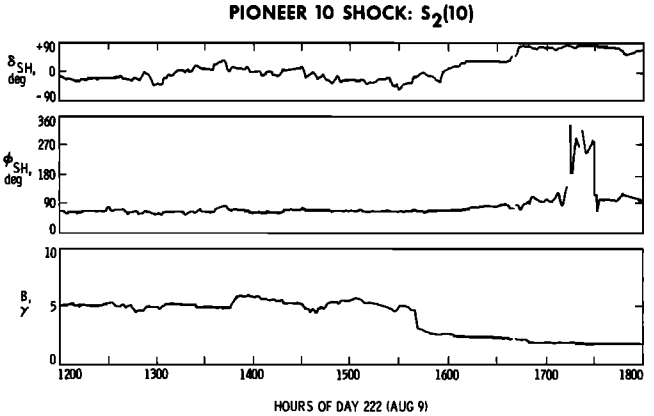

Fig. 7. Magnetic fields near the reverse shock. One-minute averages of the field magnitude and latitude and longitude are shown in the same coordinate system as is used in Figures 4–6. The reverse shock was detected at 1540 as an abrupt decrease in B accompanied by decreases in the solar wind density and temperature and an increase in velocity.

TABLE 2. Local Velocities of Pioneer 9 Shocks

Arrival at Pioneer 9							*Dryer et al.* [1976]	
Date	Time	B_1, γ	B_2, γ	V_1, km/s	V_2, km/s	V_{1n}, km/s	V_n, km/s	V_R, km/s
Aug. 3	0420	1.5	4.0	297	345	374	371	431
Aug. 3	1117	20	70	358	540	613	645	667
Aug. 4	2323	9	23	685	938	1100	1096	1183
Aug. 9	0707	8	18	403	546	660	601	672

Sonett, 1966]. However, if the shock normal is assumed to lie in or near the RT plane, then the angles between the normal and the radial direction are 14° and 23°, respectively. These results support the assumption that the shocks were propagating nearly radially at Pioneer 10.

For the third Pioneer 10 shock, on August 13, the field directions adjacent to the data gap containing the shock imply a relatively large change in direction, the included angle being 58°. The shock direction, estimated by using the coplanarity theorem, makes an angle to the radial direction of 14°. However, the angle between the normal and the upstream field direction is only 17° and deviates significantly from perpendicularity.

Although some ambiguity is inevitable because of the data gap, there is other evidence that this shock was not really quasi-perpendicular. The field upstream of the shock had a stable orientation which was more radial than azimuthal and, unless the field direction changed during the gap just prior to the shock, would not have been transverse to a radial shock normal. Under these circumstances, has a reasonably accurate velocity estimate been obtained from (1)?

The shock normal direction derived from coplanarity was used to obtain another estimate of the shock velocity corresponding to a more realistic geometry. A more general relation for the shock velocity is

$$V_{1n} = (V_{2n}B_{2t} - V_{1n}B_{1t})/(B_{2t} - B_{1t}) \quad (2)$$

in which the subscripts n and t refer to components along and transverse to the shock normal. For a perpendicular shock this relation reduces to (1).

Since the shock normal in this instance is approximately radial (to within ~14°), V_{2n} and V_{1n} are still very nearly the measured velocities upstream and downstream of the shock, i.e., 502 and 605 km/s. When these velocities and the values of the transverse magnetic field components are substituted into (2) above, it is found that V_{1n} = 616 km/s. This value compares favorably with the previous velocity estimate of 659 km/s, the difference being $\lesssim$7°. Thus this approach supports the estimate based on (1), which for the sake of simplicity and consistency is used in the subsequent discussion.

We now use these velocities, the data in Table 1, which show the times of events at the two spacecraft and of flares at the sun, and any other available clues to identify the shocks as they travel outward (Figure 10). The clearest association connects the third shock (event D) at Pioneer 10 with the fourth shock at Pioneer 9 and with the last of the four major flares (3B, W38). This shock was followed outward from the sun to the earth by the solar radio noise experiment on Imp 6 [*Malitson et al.,* 1973], was also observed at earth by Prognoz 2 [*Zastenker et al.,* 1975], and was the cause of the ssc at earth at 2354 on August 8.

Table 4 shows these local velocities, the average velocity from Pioneer 9 to Pioneer 10 based on the travel time and radial distance between the two Pioneer spacecraft, the average velocity from the sun to Pioneer 9, and the average velocity from the sun to Pioneer 10. The approximate equality of the first three of these velocities at about 650 ± 20 km/s strongly supports the view that the same shock was indeed observed at the two Pioneer spacecraft and that the shock normal was approximately radial. Furthermore, it may be concluded that there was no large change in the velocity of the shock as it propagated between 0.8 and 2.2 AU. The small discrepancy between these velocities and the average velocity from the sun to Pioneer 10 of 695 km/s and the high average velocity of 830 km/s between the sun and Pioneer 9 clearly implies that the velocity was high near the sun but that most of the deceleration had occurred by the time that Pioneer 9 was reached. There seems little point in calculating average velocities over distances as large as 2.2 AU when it is possible instead to find average velocities over distances of 0.8 and 1.4 AU.

There is also a significant difference between the above velocities and those deduced for the average speed of propagation from the sun to earth. The time between the flare and the arrival of the shock at earth implies $V(S, E)$ = 1240 km/s. A high level of confidence can be placed in this value because the shock was evidently tracked from near the sun to earth, and a velocity of 1270 km/s can be inferred from the Imp 6 radio astronomy experiment [*Malitson et al.,* 1973]. The difference between the shock speeds at Pioneer 9 and at earth may be attributed to the longitude differences between the flare site, the two Pioneer spacecraft, and earth. The shock was observed substantially earlier at earth than at 0.8 AU. Evidently, the shock front was not spherically symmetric.

TABLE 3. Local Velocities of Pioneer 10 Shocks

	Arrival at Pioneer 10							
Event	Date	Time	B_1, γ	B_2, γ	V_1, km/s	V_2, km/s	V_{1n}	V_{sw}
A	Aug. 6	1520	2.5	7.5	412	615	717	305
C	Aug. 9	1540	5	3	592	631	532	−99
D	Aug. 13	0300	1.2	3.5	502	605	659	157

There is also no ambiguity in identifying the reverse shock (event C). It was seen only at Pioneer 10, was not observed either at earth or at Pioneer 9, and hence must have developed after it passed 1 AU. As a consequence, it is not possible to compare its inertial velocity (computed from (1)) of 530 km/s and speed in the undisturbed solar wind of −99 km/s, as inferred from the Pioneer 10 measurements, with a corresponding travel time.

We now turn to the remaining shock (event A) observed by Pioneer 10 and the first three shocks observed by Pioneer 9. The situation is complicated by the fact that three shocks were observed at 0.8 AU but only one was observed at 2.2 AU and by the difficulty of determining which flare gave rise to the shock that reached Pioneer 10. Prominent features of the Pioneer 10 shock are the continued high solar wind velocity after its passage and the apparent presence of a plasma piston driver characterized by large fields of up to 16 γ. Of the four Pioneer 9 shocks, three were followed by monotonic decreases in the solar wind velocity. Only the second shock was followed by a high-speed stream, and only the second was clearly a driven shock, the driving gas being characterized by extremely large fields that approached 100 γ. (We note that $(2.2/0.8)^2(16\ \gamma) = 114\ \gamma$, although in view of the time-dependent phenomena occurring, this agreement may be accidental.) Thus we conclude that the first Pioneer 10 shock is best associated with the second Pioneer 9 shock at 1117 UT on August 3 (Figure 10).

With this identification we find an average velocity between Pioneer 9 and Pioneer 10 of 770 km/s. If the identification were made with the third shock, this average velocity would be 1460 km/s, or a value completely out of line with the local velocity estimates at Pioneer 9 and 10, as shown in Table 4. If the identification were made with the first Pioneer 9 shock, the average velocity between the two spacecraft would then be 710 km/s, and the local velocity at Pioneer 9 would be 410 km/s, a consequence which makes this identification seem unreasonable.

The identification of the first Pioneer 10 shock with the second Pioneer 9 shock implies that the average velocity from the sun to Pioneer 9 is very high, 2220 km/s. The velocity decrease between the sun and Pioneer 9 is very substantial, but, as is true in the other case, there seems to be no significant deceleration beyond Pioneer 9.

If we look more carefully at the speeds in Table 4 for the first Pioneer 10 shock, we see that the speed seems to have increased between Pioneer 9 and Pioneer 10. This could be the result of a misestimation of the local velocity at either or both spacecraft. If the effect is real, it may be the result of the second Pioneer 9 shock overtaking the first, as it should on the basis of the speeds shown in Table 2. The two shocks presumably then interacted to form a single stronger shock with a higher speed. This could explain both the increase in speed and the fact that only one shock, rather than two, was observed at Pioneer 10.

The fact that the third shock seen at Pioneer 9 was not seen at Pioneer 10 requires explanation. The characteristics of the interplanetary medium through which this shock had to propagate were strongly modified by the preceding shock and driver. The Pioneer 9 data [*Mihalov et al.*, 1974] show that the shock would have propagated into a region of extremely low density, very high temperature, and large magnetic field. All these changes would have raised the phase velocity of the fast magnetosonic wave, $(B^2/4\pi NM + \gamma kT/M)^{1/2}$, to a value in excess of the speed of this shock in the solar wind after it passed Pioneer 9, and the shock could have vanished by a subsonic transition before it reached Pioneer 10. Alternatively, the shock strength could have become so weak that the shock was not detectable.

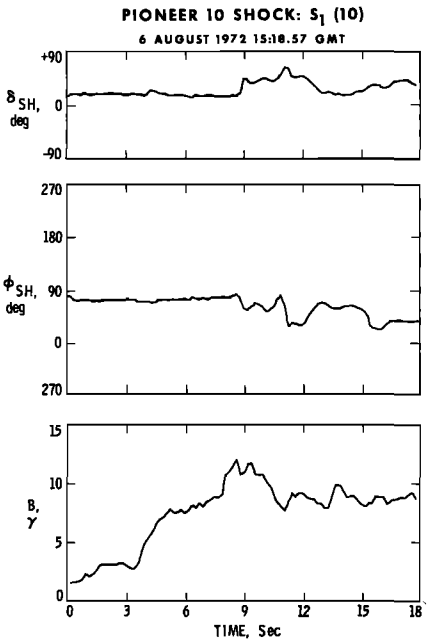

Fig. 8. Details of the first forward shock at high time resolution. The individual vector field measurements, obtained every $\frac{3}{16}$ s, are shown adjacent to the shock front. The field latitude and longitude in solar polar coordinates (described in the caption to Figure 4) appear in the upper two panels, and the magnitude is shown in the lower panel. The shock front takes approximately 2 s to pass Pioneer 10 at a speed estimated to be 717 km/s, which implies a thickness of ~1400 km.

It should be noted that other plausible shock identifications have been proposed. Independent studies of the August shocks

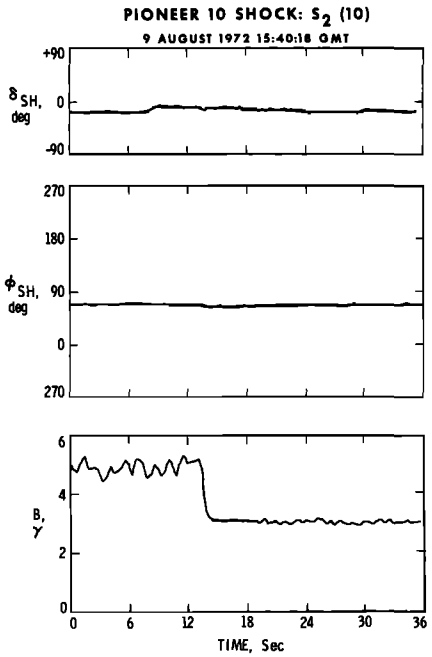

Fig. 9. Details of the reverse shock at high time resolution. The individual vector measurements, obtained every $\frac{3}{8}$ s, are shown in the same coordinates and format as are used in Figure 8. The shock was $\lesssim$500 km thick, passing Pioneer 10 in less than 1 s at a speed estimated to be 532 km/s.

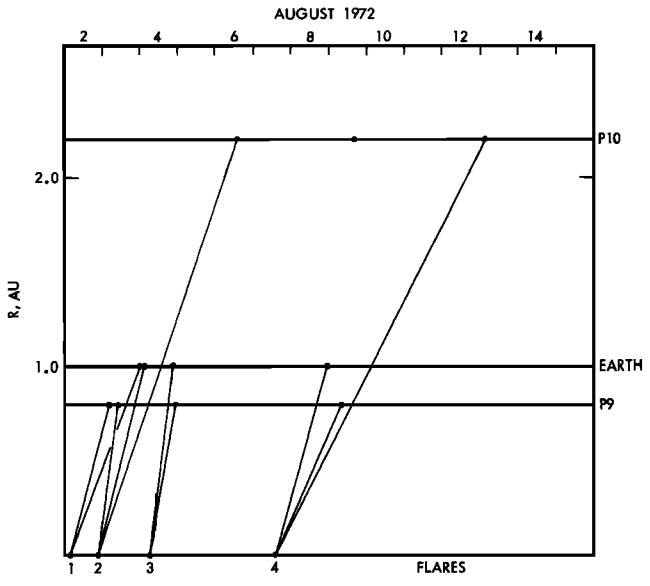

Fig. 10. Distance-time diagram showing the arrival of shocks at Pioneer 9 and 10 and at earth. The vertical axis is heliocentric radial distance, and the horizontal axis is time, the dates being given at the top of the figure. The times of occurrence of the four flares are shown along the bottom axis, where they are identified in chronological order as 1, 2, 3, and 4. The dots show the times of arrival of shocks at Pioneer 9, earth, and Pioneer 10. Straight lines connect the shocks at each location with the flare that is thought to have caused them. The slopes of these lines represent the average velocities of propagation from the sun to the point of observation. Note that although three shocks were observed at Pioneer 9 and earth in association with the first three flares, only one shock was seen at Pioneer 10 and that we associate this shock with the second flare and with the second shock at Pioneer 9 and earth.

have been carried out by *Dryer et al.* [1975] and *Zastenker et al.* [1975]. Dryer et al. present a shock characteristic diagram in which the times of arrival of the various shocks at Pioneer 9, earth, and Pioneer 10 are plotted as a function of radial distance (their Figure 9). Their identification has the first and second shocks observed at Pioneer 9 interacting slightly beyond 1 AU (as is also assumed by us). The third Pioneer 9 shock also interacts with the composite of the first two shocks before reaching Pioneer 10, so that the observation of only one shock at Pioneer 10 is accounted for (we suggest that this shock may have decayed into a large-amplitude magnetosonic wave). The basic difference between this identification and ours is that we identify the Pioneer 10 shock with a specific Pioneer 9 shock (the second), while their identification may not permit such a distinction, since the Pioneer shock is an amalgamation of the three Pioneer 9 shocks.

In a subsequent numerical simulation of the events surrounding the three flares of August 2–4, *Dryer et al.* [1976] confirmed the interaction of the shocks from flares 1 and 2 slightly beyond 1 AU. A reverse shock is also generated that could be identified with Pioneer 10 event C. However, the third shock, from flare 3, does not interact with either the forward or the reverse shock at Pioneer 10. It is perhaps significant that the time-radius diagram based on this simulation (their Figure 10) shows that the velocity of the composite of the first two Pioneer 9 shocks is essentially the same as the velocity of the second shock, which was the larger of the two. This result implies that in studying the shock propagation between Pioneer 9 and Pioneer 10, no significant error is likely to arise by identifying event A with the second Pioneer shock.

The shock identification of *Zastenker et al.* [1975] attributes the Pioneer 10 shock to the third flare and third shock seen at Pioneer 9. This identification is based principally on the plasma measurements at Pioneer 9, Pioneer 10, and earth (by Prognoz 1 and 2 and by Heos 2). It has the consequence that a relatively large deceleration of the shock is inferred between Pioneer 9 and Pioneer 10.

In contrast to *Dryer et al.* [1975] and *Zastenker et al.* [1975] we do not infer a large deceleration of either forward shock between Pioneer 9 and Pioneer 10 (Figure 11). As was mentioned above, the difference between our results and those of *Zastenker et al.* [1975] is based in part on a difference in shock identifications. However, this is not the basic reason that we draw a different conclusion from that of *Dryer et al.* [1975]. Those authors present evidence for a deceleration that is based on the behavior of average velocities of propagation of the shocks between the sun and Pioneer 9 and between the sun and Pioneer 10 (as well as between the sun and the earth). In our view a major deceleration between the sun and Pioneer 9 without any subsequent deceleration could lead to average velocities having the observed local values. Thus although we agree with *Dryer et al.* [1975] that the average velocities imply a deceleration of the shocks, we suggest that most or all of the deceleration takes place before the shocks reach 0.8 AU. It then also follows that there is little likelihood that the shocks decay into hydromagnetic waves at large heliocentric distances, as was proposed by *Dryer et al.* [1975]. It is interesting to note that as was pointed out by *Dryer et al.* [1976], their numerical simulation led to shocks that do not decelerate rapidly with distance and do not decay into hydromagnetic waves.

It should be noted that there are some unresolved ambiguities associated with our identification of the driver associated with event A. Although the Pioneer 10 shock clearly appears to be driven, there is, as was mentioned above, some uncertainty in identifying the time of arrival of the driver. There is a major change in the character of the magnetometer data at 2205 on August 6 (event B). There are lesser changes on August 7 near 0400 (a sector boundary) and near 0900 (Figure 6).

The plasma velocity rises monotonically following the shock to a maximum value of 680 km/s at ~0200 on August 7. The leading edge of the driver would be expected on physical grounds to lie within this positive velocity gradient, since the

TABLE 4. Comparison of Local and Average Shock Velocities

Arrival at Pioneer 10		Local Velocity, km/s		Average Velocity, km/s		
Date	Time	P10	P9, V_R	P9 to P10	Sun to P9	Sun to P10
Aug. 6	1520	717	667	770	2220	1000
Aug. 13	0300	659	672	635	830	695

P9 and P10 stand for Pioneer 9 and 10.

driver tends to overtake and to accelerate the gas preceding it. This expectation is borne out by numerical simulations of driven shocks [e.g., *Steinolfson et al.*, 1975]. Event B meets this condition, whereas the field changes following 0200 on August 7 occur within a region in which the velocity is monotonically decreasing. Thus the velocity data tend to favor 2205 on August 6 as the arrival time.

From Table 3 and Table 2 we see that the shock travels about 100 km/s faster than the gas behind the shock. Thus in the 76 hours from the time that the shock passed Pioneer 9 to the time that it passed Pioneer 10, 2.7×10^7 km (i.e., $76 \times 3600 \times 100$) of shocked gas would be left ahead of the driver and behind the shock. This is a lower limit, since it does not include the shocked gas that accumulated before the shock reached Pioneer 9. However, our examination of the high time resolution Pioneer 9 magnetic field data suggests that the time of arrival of the tangential discontinuity formed at the leading edge of the plasma driver was 1237 UT, or 80 min after the arrival of the shock. Since the postshock gas velocity at Pioneer 9 was 550 km/s, a distance of 2.6×10^6 km is implied, which is a negligible addition (1%) to the accumulation between Pioneer 9 and Pioneer 10. Since the plasma between the shock and the driver had a velocity of 615 km/s at Pioneer 10, we would expect the driver to arrive 12.2 hours (or $2.7 \times 10^7/615 \times 3600$) after the shock, i.e., at about 0330 on August 7. This does not agree with any of the observed field changes.

If the driver were of limited transverse extent and part of the shocked gas ahead of the driver were flowing around the sides, the shocked layer would be thinner than is expected and 2205 on August 6 could be the arrival time of the driver. The increase by 50–75 km/s of all velocities between Pioneer 9 (Table 2) and Pioneer 10 (Table 3) implies some kind of change in this layer, but it is not clear to us whether it would lead to a thickening or a thinning of the layer between the shock and the driver. It seems easier to explain a decrease of 5.5 hours in the transit time than to explain an increase of 7–12 hours.

Thickness of Pioneer 10 shocks. The available velocity information for the forward and reverse shocks at Pioneer 10 and the estimated times required for the shocks to pass the spacecraft permit the thickness of the shocks to be estimated. Figure 8 shows an approximate transit time for the forward shock of ~2 s. For a radial inertial velocity of 717 km/s the corresponding shock thickness would be ~1400 km. Figure 9 shows that the reverse shock passed the spacecraft in only $\simeq 1$ s. The thickness implied by a velocity of 530 km/s is $\simeq 500$ km. These thicknesses are larger than the typical thicknesses of the earth's bow shock [*Greenstadt et al.*, 1975].

Among the appropriate scales with which to compare these thicknesses is the preshock proton gyroradius, which is 250 km for a proton temperature of 10^6 K and $B = 1.5\ \gamma$ and 125 km for $B = 3\ \gamma$. For reasonable temperatures ($< 10^6$ K) the electron gyroradius is much smaller than the proton gyroradius (<20 km for $B = 1.5\ \gamma$). In the case of the earth's bow shock the characteristic length that is often compared with the observed shock thickness is the ion inertial length c/ω_{pi}, where ω_{pi} is the ion plasma frequency [*Greenstadt et al.*, 1975]. The proton density preceding the first shock is ~2 cm^{-3}, and the corresponding inertial length is 160 km. The proton density on the sunward side of the reverse shock is very low, $\simeq 0.2$ cm^{-3}. The ion inertial length is then 500 km. These lengths are significantly smaller than the thickness of the forward shock; however, the proton inertial length compares favorably with the thickness of the reverse shock.

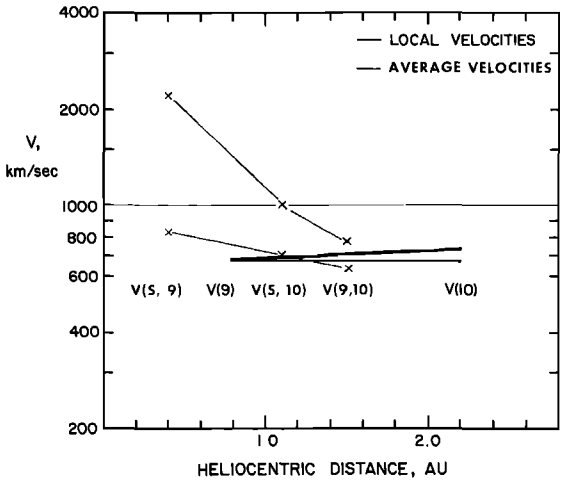

Fig. 11. Comparison of average and local shock velocities. The velocities in Table 4 are shown as a function of heliocentric distance. The gray lines connecting the average shock velocities have previously been construed to indicate a continuous deceleration of the shocks with distance. On the other hand, the dark lines which connect the local velocities at Pioneer 9 and 10 imply little, if any, deceleration between 0.8 and 2.2 AU.

SUMMARY

Using simultaneous magnetic field and plasma observations at Pioneer 10, we have identified three shocks and a plasma driver (possible flare ejecta) at 2.2 AU caused by the four large solar flares of August 2–7, 1972 (Figures 2 and 3). Two shocks, the first and third, were forward shocks, while the second was a reverse shock. The local inertial velocities of all three shocks have been estimated (Table 3) by using the magnetic field and solar wind velocity observations under the assumption of quasi-perpendicularity; i.e., the shocks were assumed to be propagating principally across, rather than along, the interplanetary field.

The local velocity (659 km/s) of the last Pioneer 10 shock from the fourth flare agrees very well with the local velocity at Pioneer 9 (672 km/s) and with the average velocity between the two Pioneer spacecraft of 635 km/s (Figure 11). Both local velocities, however, are significantly smaller than the average velocities of propagation (Table 4) from the sun to Pioneer 9 (830 km/s), to Pioneer 10 (695 km/s), and to earth (1240 km/s), which were previously used by other authors to identify corresponding shocks at different locations and which led to the conclusion that the shocks were continuously decelerating as they propagated outward from the sun. The approximate equality of the local shock speeds at Pioneer 9 and 10 with the average velocity over this range implies little, if any, deceleration of the shock between 0.8 and 2.2 AU. The difference between the local and the average velocities from the sun to the spacecraft, the local velocity being significantly smaller than the average velocities, is consistent with the deceleration of the shock after it leaves the sun but substantially before it reaches 0.8 AU.

The identification of corresponding shocks at Pioneer 9 and 10 associated with the first three flares has been reinvestigated (Figure 10). Three forward shocks were observed at Pioneer 9, but only one shock was subsequently seen at Pioneer 10, implying a strong mutual interaction before the shocks reached 2.2 AU. On the assumption that the Pioneer 10 shock is driven we identify the Pioneer 10 shock with the only driven shock at Pioneer 9, which was the second and largest shock. It

is presumed that the second, higher-velocity shock at Pioneer 9 overtook the first, slower shock before it reached Pioneer 10, thus causing the shock from the first flare to be absent at Pioneer 10. We also suggest that the third Pioneer 9 shock did not reach Pioneer 10, possibly because it interacted with the shock preceding it. Another possibility is that as the shock propagated into the postshock gas and flare ejecta associated with the preceding driven shock, it underwent a transition back into a large-amplitude hydromagnetic wave.

The identification of the second shock at Pioneer 9 with the first shock at Pioneer 10 leads to reasonably good agreement between the local velocities at Pioneer 9 (670 km/s) and Pioneer 10 (720 km/s) as well as with the average propagation speed from Pioneer 9 to Pioneer 10 (770 km/s). These velocities (Figure 11), however, are again significantly slower than the average velocities from the sun to Pioneer 9 (2220 km/s) and Pioneer 10 (1000 km/s). We again attribute these differences between the local and average speeds to a major deceleration of this shock as it propagates outward from the sun. However, the direct comparison of the local shock speeds with the average speed between the two spacecraft, which shows them to be approximately equal, again implies the absence of significant deceleration from 0.8 AU outward.

Thus we conclude from these observations of flare-produced shocks, the first observed at distances well beyond 1 AU, that the shocks tend to be propagating at approximately constant velocity by the time that they reach the orbit of earth. The observations are consistent with numerical simulations such as those of *Hundhausen* [1973] and *Dryer et al.* [1975], which show only a slight deceleration beyond 1 AU.

The thicknesses of the first forward shock (Figure 8) and the reverse shock (Figure 9) were computed from the local shock speeds and the times required for the shocks to pass the spacecraft. The thicknesses were also compared with characteristic plasma parameters such as the proton gyroradius and inertial length. The forward shock appears to be relatively thick (~1400 km) in comparison with anticipated values of both the proton gyroradius (250 km) and the inertial length (160 km). The reverse shock is significantly thinner (≃500 km), and its thickness compares favorably with the proton inertial length (estimated to be 500 km).

Acknowledgments. We are grateful to John Wolfe for providing us with the Pioneer 9 and 10 solar wind velocities and to Devrie Intriligator for the high-resolution Pioneer 10 velocities. We benefited from discussions of the August shocks with them and with Murray Dryer. Charles Sonett and David Colburn provided the high-resolution magnetic field data from their Pioneer 9 investigation for use in computing local velocities. Elaine Parker of the Jet Propulsion Laboratory assisted in the reduction of the magnetic field data. The thoughtful comments of the two referees were very helpful. This report represents one aspect of research carried out by the Jet Propulsion Laboratory for the National Aeronautics and Space Administration under contract NAS7-100. Support for Leverett Davis, Jr., was provided by NASA grant NGR-0-5-002-160.

The Editor thanks M. Dryer and K. W. Behannon for their assistance in evaluating this paper.

REFERENCES

Burlaga, L. F., A reverse hydromagnetic shock in the solar wind, *Cosmic Electrodynamics, 1,* 233, 1970.

Chao, J. K., and R. P. Lepping, A correlative study of ssc's, interplanetary shocks, and solar activity, *J. Geophys. Res., 79,* 1799, 1974.

Colburn, D. S., and C. P. Sonett, Discontinuities in the solar wind, *Space Sci. Rev., 5,* 439, 1966.

Dryer, M., Interplanetary shock waves—Recent developments, *Space Sci. Rev., 17,* 277, 1975.

Dryer, M., A. Frohlich, A. Jacobs, J. H. Joseph, and E. J. Weber, Interplanetary shock waves and comet brightness fluctuations, *J. Geophys. Res., 80,* 2001, 1975.

Dryer, M., Z. K. Smith, R. S. Steinolfson, J. D. Mihalov, J. H. Wolfe, and J. K. Chao, Interplanetary disturbances caused by the August 1972 solar flares as observed by Pioneer 9, *J. Geophys. Res., 81,* 4651, 1976.

Fairfield, D. H., Whistler waves observed upstream from collisionless shocks, *J. Geophys. Res., 79,* 1368, 1974.

Gosling, J. T., J. R. Asbridge, S. J. Bame, A. J. Hundhausen, and I. B. Strong, Satellite observations of interplanetary shock wave, *J. Geophys. Res., 73,* 43, 1968.

Greenstadt, E. W., Structure of the terrestrial bow shock, in *Solar Wind Three,* edited by C. T. Russell, p. 440, University of California, Los Angeles, 1974.

Greenstadt, E. W., C. T. Russell, F. L. Scarf, V. Formisano, and M. Neugebauer, Structure of the quasi-perpendicular laminar bow shock, *J. Geophys. Res., 80,* 502, 1975.

Hirshberg, J., A. Alksne, D. S. Colburn, S. J. Bame, and A. J. Hundhausen, Observations of a solar flare induced interplanetary shock and helium-enriched driver gas, *J. Geophys. Res., 75,* 1, 1970.

Hundhausen, A. J., Composition and dynamics of the solar wind plasma, *Rev. Geophys. Space Phys., 8,* 729, 1970.

Hundhausen, A. J., *Solar Wind and Coronal Expansion,* Springer, New York, 1972.

Hundhausen, A. J., Evolution of large-scale solar wind structures beyond 1 AU, *J. Geophys. Res., 78,* 2035, 1973.

Hundhausen, A. J., and R. A. Gentry, Numerical simulations of flare-generated disturbances in the solar wind, *J. Geophys. Res., 74,* 2908, 1969.

Intriligator, D. S., Pioneer 9 and Pioneer 10 observations of the solar wind associated with the August 1972 events, submitted to *J. Geophys. Res.,* 1976.

Malitson, H. H., J. Feinberg, and R. G. Stone, A density scale for the interplanetary medium from observations of a type 2 solar radio burst out to one astronomical unit, *Astrophys. J., 183,* L35, 1973.

Mihalov, J. D., D. S. Colburn, H. R. Collard, B. F. Smith, C. P. Sonett, and J. H. Wolfe, Pioneer solar plasma and magnetic field measurements in interplanetary space during August 2–17, 1972, in *Correlated Interplanetary and Magnetospheric Observations,* edited by D. E. Page, D. Reidel, Dordrecht, Netherlands, 1974.

Parker, E. N., Sudden expansion of the corona following a large solar flare and the attendant magnetic field and cosmic ray effects, *Astrophys. J., 133,* 1014, 1961.

Smith, E. J., B. V. Connor, and G. T. Foster, Jr., Measuring the magnetic field of Jupiter and the outer solar system, *IEEE Trans. Magn., MAG-11,* 962, 1975.

Sonett, C. P., and D. S. Colburn, The si^+, si^- pair and interplanetary forward-reserve shock ensembles, *Planet. Space Sci., 13,* 675, 1965.

Sonett, C. P., D. S. Colburn, L. Davis, Jr., E. J. Smith, and P. J. Coleman, Jr., Evidence for a collision-free magnetohydrodynamic shock wave in interplanetary space, *Phys. Rev. Lett., 13,* 153, 1964.

Steinolfson, R. S., M. Dryer, and Y. Nakagawa, Numerical MHD simulation of interplanetary shock pairs, *J. Geophys. Res., 80,* 1223, 1975.

Wolfe, J. H., J. D. Mihalov, H. R. Collard, D. D. McKibbin, L. A. Frank, and D. S. Intriligator, Pioneer 10 observations of the solar wind interaction with Jupiter, *J. Geophys. Res., 79,* 3489, 1974.

World Data Center A for Solar-Terrestrial Physics, Collected data reports on August 1972 solar-terrestrial events, *Rep. UAG-28,* Boulder, Colo., 1973.

Zastenker, G. N., O. L. Vaisberg, F. Cambou, V. V. Temny, and M. Z. Khokhlou, Propagation of solar-flare-generated shock waves in August 1972 by solar wind measurements, paper presented at COSPAR Meeting, Space Res. Inst., Acad. Sci. USSR, Varna, Bulgaria, June 2–7, 1975.

(Received May 10, 1976;
accepted October 14, 1976.)